

Article

Co-Location Potential of Floating PV with Hydropower Plants: Case Study in Ecuador

Carlos D. Rodríguez-Gallegos ^{1,*} , Oktoviano Gandhi ², César A. Rodríguez-Gallegos ³
and Manuel S. Alvarez-Alvarado ⁴

¹ RINA Tech Renewables Australia, RINA Consulting, Melbourne, VIC 3000, Australia

² Solar Energy Research Institute of Singapore (SERIS), National University of Singapore (NUS), Singapore 117574, Singapore

³ Department of Mechanical and Industrial Engineering, Concordia University, Montreal, QC H3G 1M8, Canada

⁴ Faculty of Electrical and Computer Engineering, Escuela Superior Politécnica del Litoral (ESPOL), Guayaquil EC090112, Ecuador

* Correspondence: cardarod88@gmail.com

Abstract: This study explores the potential for co-locating floating photovoltaics (FPVs) with existing hydropower plants (HPPs) in Ecuador. Ecuador's heavy reliance on hydropower for electricity generation, combined with recent blackouts caused by prolonged dry seasons, underscores the importance of diversifying energy sources. The integration of FPVs with HPPs offers a promising opportunity to enhance energy security by reducing dependency on a single energy source and improving economic, electrical, and environmental outcomes. In this paper, we assess all HPPs in Ecuador and quantify the potential performance of FPV systems when installed at their sites. Our results show that FPV systems can not only contribute additional electricity to the grid but also improve HPP performance by reducing water evaporation from reservoirs and maintaining generation capacity during dry seasons, when solar irradiation is typically higher. To model the energy production, yield, and performance of the FPV systems, we applied RINA's methodology to estimate representative weather conditions for each site and simulate FPV performance, accounting for system design loss factors. Additionally, we calculated the water savings resulting from FPV installation. Our findings reveal that, out of approximately 70 HPPs in Ecuador, 11 present favorable conditions for large-scale FPV deployment. Among these, Cumbayá HPP (40 MW) exhibited the most suitable conditions, supporting a maximum FPV capacity of 17 MWp. Marcel Laniado de Wind HPP (213 MW) and Mazar HPP (170 MW) were also identified as optimal candidates, each with potential FPV capacities equal to their installed HPP capacities. While this study primarily aims to provide scientific evidence on the potential of FPV-HPP co-location, the results and methodology can also guide Ecuadorian government authorities and investors in adopting FPV technology to strengthen the country's energy infrastructure.

Keywords: floating photovoltaics; hydropower plants; co-location assessment; electrical performance; water savings



Academic Editor: Jürgen Heinz Werner

Received: 25 September 2024

Revised: 30 January 2025

Accepted: 3 February 2025

Published: 4 February 2025

Citation: Rodríguez-Gallegos, C.D.; Gandhi, O.; Rodríguez-Gallegos, C.A.; Alvarez-Alvarado, M.S. Co-Location Potential of Floating PV with Hydropower Plants: Case Study in Ecuador. *Solar* **2025**, *5*, 3. <https://doi.org/10.3390/solar5010003>

Copyright: © 2025 by the authors. Licensee MDPI, Basel, Switzerland. This article is an open access article distributed under the terms and conditions of the Creative Commons Attribution (CC BY) license (<https://creativecommons.org/licenses/by/4.0/>).

1. Introduction

Hydropower plants (HPPs) serve as a key source of electricity for many countries, particularly those with favorable natural conditions such as high-altitude reservoirs or regions where infrastructure has been developed to harness hydropower [1–3]. Ecuador,

located in South America, is one such country, where HPPs play a central role in electricity generation. By 2023, approximately 80% of Ecuador's electricity was generated by HPPs [4], underscoring the critical importance of these systems to the nation's energy supply.

While HPPs are a renewable and reliable energy source, they have inherent limitations; i.e., their availability is reduced significantly during dry seasons [5,6]. This limitation became starkly evident recently when severe dry seasons led to multiple power outages across the country. Since October 2023, planned blackouts have been implemented in various provinces to conserve water in HPP reservoirs [7,8]. However, unforeseen blackouts have also occurred, such as the nationwide outage on 19 June 2024, which lasted over three hours. This disruption was attributed to a failure in the Milagro–Zhoray transmission line, compounded by a storm that affected two of Ecuador's largest hydropower plants—Coca Codo Sinclair and Agoyán—during which sediment washed into the facilities, forcing the turbines to shut down [9].

Ecuador's current energy challenges highlight the urgent need to diversify its energy sources to increase its robustness in different and extreme weather conditions, as well as enhance grid resilience [10–14]. In this context, we explore the potential benefits of installing floating photovoltaic (FPV) systems [15] on HPP reservoirs within Ecuador.

Photovoltaic (PV) systems were selected for this study due to their rapid global deployment in recent years, driven by technological advancements and declining costs, making them an attractive option for energy projects worldwide [16]. Moreover, Ecuador has significant solar irradiance, further supporting the feasibility of solar energy systems. Among the various PV installation types, e.g., [17–22], FPV systems were chosen for their potential to complement HPPs. By installing FPV systems on hydropower reservoirs, both energy sources stand to benefit—an idea that this study seeks to explore and quantify. Details on the challenges associated with FPV can be found in [23].

While previous research have explored the potential of integrating multiple energy sources including the combination of FPV systems with HPP [24–26], numerous studies have primarily focused on specific geographic regions or limited datasets. Notable studies have investigated the synergy between FPVs and HPPs in various contexts, demonstrating the feasibility and advantages of such integration in optimizing renewable energy generation and resource use [27,28]. However, the scope of these studies has been somewhat limited in terms of data diversity and regional application. In contrast, our study, to the best of our knowledge, represents the first comprehensive attempt to evaluate the co-location of FPV systems with hydropower plants using a complete and nationwide dataset of HPPs in a country like Ecuador, employing state-of-the-art methodologies to predict the electrical and water savings potential. Ecuador, which is heavily dependent on hydropower for its electricity generation, offers a unique and valuable case for exploring how this combination of technologies can enhance the country's energy landscape.

Ecuador's energy mix is primarily dominated by hydropower, with a significant portion of the country's electrical demand being met through its vast hydropower resources. However, the nation also faces challenges such as seasonal variability in water availability and periods of drought that can impact the reliability of hydropower. By integrating FPV systems with HPPs, there is a potential to mitigate some of these challenges and increase the overall efficiency and resilience of the national power grid. FPV systems, when deployed on water bodies associated with hydropower plants, can not only contribute to power generation but also improve the overall performance of the hydropower plants by reducing water evaporation and increasing the energy yield from both sources.

In our research, we have employed industry-recognized software tools in combination with RINA's established methodology to simulate the performance of FPV systems with high precision. This simulation framework has allowed us to assess the technical, economic,

and environmental benefits of FPV installations in real-world scenarios, using reliable data from Ecuador's hydropower infrastructure. Through these simulations, we have quantified several key impacts, including the potential for water conservation. FPV systems, by shading the water surface, can significantly reduce evaporation rates, which is especially crucial in regions where water scarcity and climate change pose growing threats to the stability of hydropower generation.

Furthermore, this study goes beyond merely assessing the technical viability of FPV integration. It also highlights the broader implications for energy security and sustainability. By enhancing the capacity for power generation and improving the stability of hydropower operations, FPV systems can help diversify Ecuador's renewable energy portfolio, thereby strengthening the country's energy security. This becomes especially pertinent as global energy markets face increasing pressure to transition to renewable sources, and nations like Ecuador seek to reduce their dependence on fossil fuels while ensuring a reliable energy supply.

Our research aims to provide valuable insights into how FPV systems can play a pivotal role in enhancing the energy security, reliability, and sustainability of Ecuador's power sector. The findings of this study can offer crucial information for a wide range of stakeholders, including government officials, policymakers, energy investors, and researchers. Government bodies and policymakers can utilize this knowledge to develop more informed, forward-thinking strategies to encourage the adoption of FPV technologies as part of the country's broader energy transition goals. Investors can gain a clearer understanding of the financial and environmental benefits of investing in FPV systems in conjunction with existing hydropower assets. Moreover, the research contributes to the global academic and scientific dialogue on renewable energy integration, offering a valuable case study for other nations with similar hydropower-dominated energy systems.

Ultimately, the results of this study can serve as a springboard for future research into the integration of FPV systems with other forms of renewable energy, exploring the synergies and trade-offs involved in optimizing diverse energy resources for enhanced sustainability. By focusing on real-world data and comprehensive simulations, our work sets the stage for the widespread adoption of hybrid renewable energy systems that can address both current and future challenges in energy production and environmental conservation.

The remainder of this paper is structured as follows: Section 2 provides a summary of the HPPs located in Ecuador; Section 3 discusses the advantages of HPP-FPV co-location; Section 4 outlines the methodology used to estimate weather conditions, FPV electrical performance and water savings. Furthermore, Section 5 details the case study, and the results are provided and discussed in Section 6. Finally, Section 7 summarizes the conclusions from this study and future works.

2. HPPS Deployed in Ecuador

As highlighted in the Introduction, Ecuador is heavily reliant on hydropower plants (HPPs) to meet its electricity demand. The country has approximately 70 HPPs [4], each with distinct characteristics, such as turbine type and technology, reservoir size, and transmission line interconnections. These HPPs vary widely in capacity, with the largest, Coca Codo Sinclair, boasting a capacity of 1500 MW, while the smallest, Tanque Alto Carcelén, has a capacity of just 0.06 MW.

According to the 2023 Annual Report from the Ecuadorian National Operator of Electricity (CENACE) [4], Ecuador imported 1.3 TWh of electricity in 2023. Meanwhile, domestic electricity production totaled 32 TWh, with 25 TWh generated by HPPs, 5 TWh by thermal power plants, and 0.5 TWh from renewable sources such as wind, biomass, PV

systems, and biogas. These figures underscore the central role that HPPs play in Ecuador's energy system.

Figure 1a illustrates the number of HPPs in Ecuador, categorized by their installed capacity. It is evident that most of these plants are relatively small in size. However, as shown in Figure 1b, the total energy production in 2023 reveals that the majority of the country's electricity generation is concentrated among a few large-scale HPPs.

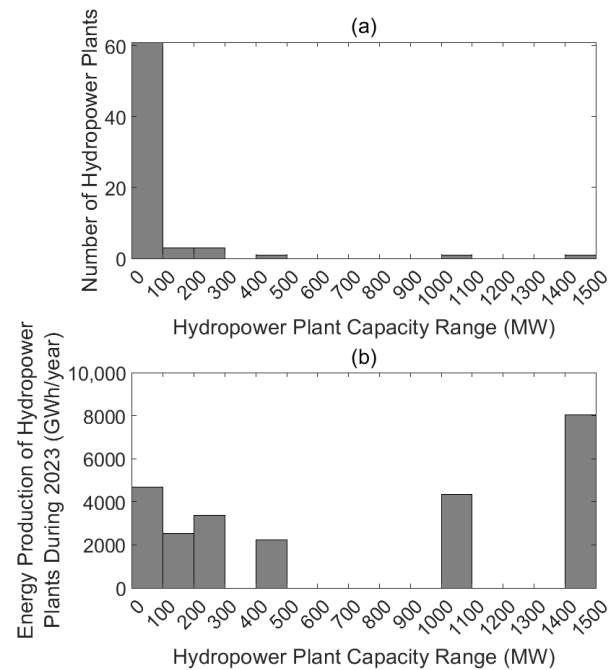


Figure 1. Histograms based on the hydropower capacities for (a) number of HPP plants, and (b) 2023 annual energy production.

Figure 2 then shows the location of the HPP plants across Ecuador, where the size of the circles represents their installed capacity. This figure highlights how most of the HPPs are of small size, while only three are larger than 400 MW. In addition, this figure highlights that most of the hydropower plants are installed in the Ecuadorian highlands, which is expected, as this region is composed of reservoirs located at different altitudes and thus can be used for HPP applications.

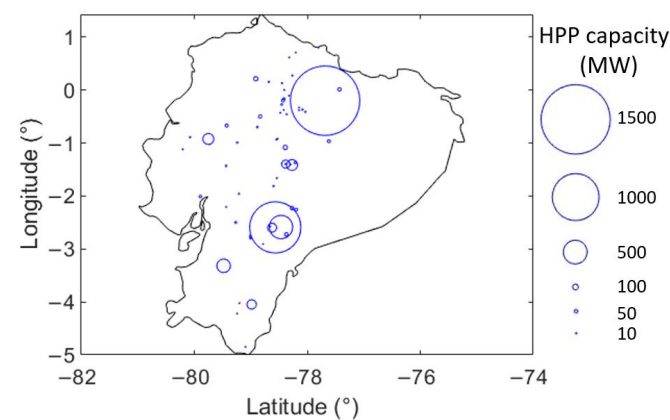


Figure 2. Hydropower plants' locations in Ecuador. The circle size is linearly increased to represent the hydropower plant installation capacity, where the largest circle shows the 1500 MW capacity from Coca Codo Sinclair. Negative latitude values refer to the Western hemisphere, while positive longitude values refer to the Northern hemisphere.

3. Co-Location of FPV with HPP

FPV systems were selected in this study as a valuable addition to Ecuador's energy portfolio. Beyond generating electricity, FPV installations on HPP reservoirs offer several key advantages. When FPV systems are deployed at sites where HPPs already exist and operate independently, this arrangement, known as FPV-HPP co-location, presents the following benefits:

- **Infrastructure Efficiency:** Since HPPs are already fully connected to the electrical grid, the same infrastructure can be used by FPV systems to feed electricity into transmission lines. This reduces FPV installation costs and optimizes the use of existing grid capacity by increasing the total energy output. Additionally, other shared infrastructure, such as access roads, can be utilized for both HPP and FPV systems, simplifying installation and maintenance.
- **Water Conservation:** FPV systems, consisting of solar panels mounted on floating platforms, partially block sunlight from reaching the water surface, reducing evaporation [29]. This helps retain more water in reservoirs, which can then be used to generate electricity during times of need.
- **Seasonal Synergy:** HPPs often face challenges during prolonged dry seasons due to reduced water availability in their reservoirs. FPV systems can help offset this by generating more electricity during dry periods, which are typically associated with high solar irradiance. Conversely, during the rainy season, while FPV energy production may decline, HPPs can generate ample electricity due to increased water availability. This seasonal complementarity enhances overall energy reliability.
- **Increased Capacity:** Expanding the energy production of HPPs often requires constructing additional dams, which can raise environmental concerns. While FPV systems also have environmental impacts that must be assessed, they may offer a more environmentally friendly alternative for boosting total energy production by leveraging existing water surfaces without the need for new infrastructure.
- **Environmental Benefits:** By shading parts of the water, FPV systems can reduce or prevent algae blooms, which can improve water quality and the overall ecological conditions of the reservoir [30].

4. FPV Modeling and Simulations

The objective of this paper is to analyze and quantify the impact of installing FPV systems on water bodies utilized by existing HPPs. This section outlines the key factors considered in the simulations. We begin by detailing the process of acquiring critical weather data, specifically solar irradiance and temperature, which are essential for predicting the energy potential of FPV systems. Following this, we calculate the expected water savings resulting from FPV installations, based on their ability to reduce evaporation from the reservoirs.

4.1. Estimation of Weather Conditions

To predict the annual weather conditions for the selected locations, where FPV systems are assumed to be installed, we employ RINA's weighted mean methodology. This approach integrates multiple databases, assigning weights to each to derive a representative set of weather conditions, thereby minimizing potential inaccuracies associated with individual sources.

The employed methodology utilizes two weighting factors for each database: one based on spatial resolution and the other on temporal resolution. Specifically, databases closer to the site of interest and those with a greater number of historical data years receive higher weighting factors in the mean calculation. This process ultimately produces a

Typical Meteorological Year (TMY) dataset, which will be used in the simulations detailed in subsequent sections. Additional information on this methodology can be found in [31].

For this study, we selected three databases: Meteonorm (combining satellite and ground-based data) [32], Solargis (satellite-based) [33], and the National Solar Radiation Database (NSRDB) (also satellite-based) [34], as they are anticipated to provide a reliable representation of weather conditions in the region. Table 1 below outlines their spatial and temporal resolutions for locations in Ecuador:

Table 1. Spatial and temporal resolution per weather database for Ecuador.

Database	Spatial Resolution (km)	Number of Years
Meteonorm	8	20 (1996–2015)
Solargis	1	25 (1999–2023)
NSRDB	4	25 (1998–2022)

Figure 3 below illustrates the calculation process. It is important to note that while combining multiple datasets offers advantages in reducing the impact of potential inaccuracies from individual datasets, the calculated irradiance is determined by considering the weighted influence of spatial resolution and the number of years for each dataset. This approach ensures that datasets providing more reliable insights into the studied site are given greater priority in the final calculation.

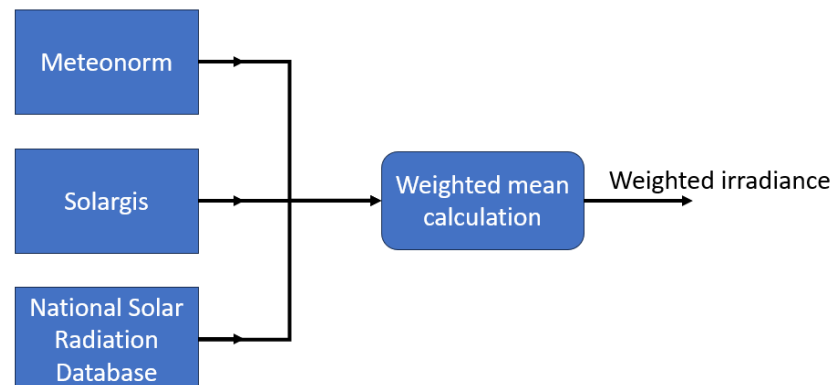


Figure 3. Graphical representation of the weighted mean calculation used to estimate the representative irradiance for the site of interest, accounting for spatial resolution and dataset duration.

4.2. FPV Electricity Production

Once the representative Typical Meteorological Year (TMY) weather conditions are established for each site of interest, the next step is to calculate the expected energy potential from floating photovoltaic (FPV) systems. We simulated the performance using PVsyst Version 7 [35], a commercial software widely recognized in both industry and research, enhancing the reliability of our results for future implementations. Additionally, RINA's methodology was employed to define the various loss factors associated with the PV system, supplemented by RINA's in-house tool for more precise calculations of certain system losses. RINA Consulting is a leading consulting firm that specializes in renewable energy systems, including photovoltaic (PV) technologies, wind farms, battery energy storage systems (BESS), and hydrogen solutions. Drawing on our extensive experience and research and development efforts from numerous projects worldwide, we have estimated the expected loss values to be used in these simulations considering large-scale PV systems.

For the FPV systems, the following criteria were considered:

- **Tilt and Orientation:** The general guideline for PV installations is to align the tilt with the latitude of the location, facing the equator [36,37]. However, since Ecuador's

latitude ranges from 1.5° to -5.1° , this guideline's effectiveness diminishes. Many module manufacturers recommend a minimum tilt of 10° to facilitate self-cleaning during rainfall [38,39]. Therefore, we assume that the FPV systems will be installed at a 10° tilt, oriented towards the direction yielding the highest irradiance collection as determined by PVsyst (North/South/East/West).

- **Bifacial Panels:** This study will utilize bifacial panels, which can capture irradiance from both sides. However, the additional rear-side irradiance gain is minimal for FPV installations near the equator, due to low tilt angles, proximity to water, and low water albedo [37,40,41]. Furthermore, rear-side irradiance is absorbed with a lower conversion efficiency (typically between 65% and 85% for current industrial panels). The sun's path near the equator also limits the irradiance reaching the panel's rear side [36], leading us to neglect rear-side contributions in this analysis. Nonetheless, bifacial panels are still advantageous in FPV systems due to their glass/glass construction, which helps mitigate degradation compared to glass/backsheet monofacial panels [21].
- **Design Configuration:** The simulations assume a landscape orientation for the FPV system, featuring rows of single panels. Each row is positioned between floating platforms to allow easy access for operation and maintenance. Given the installation on water, the terrain is presumed flat, and the low panel tilt minimizes potential shading losses from adjacent PV rows, which are therefore not considered in this analysis.
- **Cooling Effects:** Research indicates that FPV systems may outperform land-based PV systems due to enhanced cooling effects, which can reduce temperature-related losses [42–44]. Factors contributing to this cooling include higher wind profiles above water bodies and water evaporation, which can create cooling mist. For this study, we assume a yield boost of 6% based on findings from [45].
- **Mismatch Losses:** Since the panels are mounted on floating platforms, their orientation may shift over time due to water movement, causing panels in the same string to receive varying amounts of irradiance. This leads to mismatch losses, which occur when the panel with the lowest irradiance limits the power production of the others from the same PV string. We estimate these losses at 3%, based on [46], considering medium wave intensity to account for the water body behavior and HPP influence.
- **Soiling Losses:** We estimate soiling losses using RINA's in-house tool, factoring in the yearly rainfall profile and the assumption of one manual cleaning per year as part of O&M services. While shading losses due to bird droppings are a concern [47,48]—especially in natural areas—addressing this requires a detailed study of local bird behavior, which is beyond the scope of this work. Further details on soiling studies can be found in [49,50].

RINA's methodology, grounded in extensive R&D activities and global industrial experience with large-scale PV systems, is employed to characterize the loss factors impacting the PV systems. This study calculates the performance of the FPV systems up to the medium/high voltage transformer, where generated power will be injected into the transmission line. The results provide a comprehensive overview of the expected performance and energy production destined for the national grid.

The electrical performance assessment will focus on three key properties:

1. **Energy Production (GWh/year):** This represents the total energy expected to be injected into the transmission line, calculated as:

$$E = \sum_i P_i \Delta t \quad (1)$$

where P_i [MW] is the power injected into the grid at time step i , and Δt [h] is the duration of the time step.

The power calculation is based on the weather and system characteristics for a given time step. This can be expressed using the following equation, which serves as a general reference for the power calculations in this manuscript. The power is calculated using PVsyst software and RINA's in-house tools:

$$P_i = \frac{P_{PV}}{1000} I [1 + \gamma (T_c - 25^\circ\text{C})] (1 - l_1) (1 - l_2) (1 - l_3) \cdots (1 - l_n) \quad (2)$$

In this equation, P_{PV} [Wp] represents the total power output of the installed modules under standard test conditions (STC), and I [A] denotes the total irradiance reaching the solar panels. The second term accounts for the temperature effect on module performance, where γ [%/°C] is the power temperature coefficient, and T_c [°C] is the cell temperature. The remaining factors, l_1, l_2, \dots, l_n , represent various loss factors, including those due to reflection, degradation, ohmic losses, and losses from the inverter and transformer, among others.

2. Performance Ratio PR (%): This metric measures the ratio of measured (or simulated) energy production to ideal energy production, defined as:

$$PR = \frac{\sum_i P_i \Delta t}{\sum_i P_{STC} \frac{I_i \Delta t}{1000\text{W}/\text{m}^2}} 100\% \quad (3)$$

where P_{STC} [MWp] is the installation capacity of the FPV system, and I_i [W/m²] is the irradiance reaching the solar panels at time step i . PR serves as an indicator of the system's health.

3. Yield (kWh/kWp): This represents the annual electricity production injected into the grid relative to the FPV installation capacity. It combines the previous two metrics and is crucial for understanding the efficacy of the FPV system, calculated as:

$$Yield = \frac{E}{P_{STC}} \quad (4)$$

$$Yield = \frac{PR}{100\%} \sum_i \frac{I_i}{1000\text{W}/\text{m}^2} \quad (5)$$

4.3. FPV Water Savings

Given that the FPV system is installed on water, we anticipate water savings resulting from reduced evaporation. The system blocks a portion of sunlight that would otherwise reach the water's surface, potentially extending the operational capacity of hydropower plants by maintaining higher water levels in their reservoirs.

To quantify the volume of water that does not evaporate due to the influence of the FPV system, we define ΔE_v [m³] using the following equation:

$$\Delta E_v = E_v A \varepsilon \quad (6)$$

where E_v [m/day] is the daily evaporation rate, A [m²] is the area of the FPV system, and ε [%] represents the evaporation reduction efficiency attributable to the FPV installation. In this study, ε is set at 60.2%, based on findings from [29].

To calculate E_v , we employ the equation proposed by Linacre [51]:

$$E_v = \frac{700 \frac{(T_a + 0.006 e_i)}{100 - \Phi} + 15 (T_a - T_d)}{80 - T_a} \quad (7)$$

where T_a [$^{\circ}\text{C}$] is the ambient temperature, e_l [m] is the site elevation, Φ [$^{\circ}$] is the latitude, and T_d [$^{\circ}\text{C}$] is the dew-point temperature.

5. Case Study

In this analysis, we consider a representative FPV system based on current market conditions. The selected solar panel technology is crystalline silicon half-cell n-type bifacial, paired with a central inverter—both of which are commonly utilized in large-scale PV farm projects. The specific models for the solar panel and inverter were sourced from leading manufacturers, recognized for their high shipping volume in 2024. The identity of the manufacturers is not disclosed in this paper, as the focus is on the typical characteristics of these technologies to create a representative system. The key electrical properties of the selected equipment are summarized in Table 2 below:

Table 2. Properties of selected solar panel and inverter.

Solar Panel Properties Under Standard Testing Conditions			
Power	625 W _p	Bifaciality	80%
Maximum power voltage	46.1 V	Maximum power current	13.56 A
Open circuit voltage	55.72 V	Short circuit current	14.27 A
Power temperature coefficient	−0.29%/ $^{\circ}\text{C}$	Efficiency	22.36%
Inverter properties			
DC MPP voltage range	800–1300 V	Maximum PV input current	7016 A
AC power	4950 kVA	Maximum AC current	5200 A
AC voltage	10–35 kV	Frequency	50, 60 Hz
Total harmonic distortion	<3%	Maximum/European efficiency	99.0/98.7%

The FPV system analyzed in this study is a typical pure-float FPV configuration, consisting of high-density polyethylene floaters on which solar panels are mounted. Figure 4 illustrates this system. This type of FPV system is the one mostly employed in the industry currently. For the calculation of the installed capacity of the FPVs, we assume that 1 hectare is required to install 1 MW_p of FPV. This ratio is expected to decrease over time as solar panel efficiency improves and FPV design evolves, but it remains within the current range for typical FPV installations.



Figure 4. Illustration of the typical pure-float FPV system which is considered in this study.

Ecuador currently has around 70 hydropower plants (HPPs) across the country. For this study, we selected the HPPs most likely to benefit from co-locating with an FPV system, based on the following criteria:

- HPPs must have an installed capacity of at least 15 MW to ensure that the FPV system can achieve significant capacity, which may be implemented in multiple phases if necessary. As the same transmission line capacity is shared, it is assumed that the installation capacity of the FPV system shall not exceed the HPP capacity.

- The water bodies associated with the HPPs should have sections at least 100 m wide, as these areas will be designated for the FPV installation, and proper space needs to be assured to deploy sizable FPV systems.
- The water bodies must be in close proximity to the HPP to minimize potential transmission losses and costs associated with the FPV system.

Based on these criteria, we identified a total of 11 HPPs for this study, as detailed in Table 3 below.

Table 3. Properties of selected HPPs with favorable conditions for FPV deployment. Negative latitude values refer to the Western hemisphere, while positive longitude values refer to the Northern hemisphere.

HPP	Capacity (MW)	Energy Production in 2023 (GWh)	Latitude (°)	Longitude (°)
Coca Codo Sinclair	1500	8033	−2.591	−78.567
Paute	1100	4334	−3.317	−79.481
Minas San Francisco	270	995	−0.923	−79.752
Marcel Laniado de Wind	213	1123	−1.414	−78.270
Mazar	170	554	−1.398	−78.383
Agoyán	154	963	−1.082	−78.390
Pucará	70.6	188	0.215	−78.911
Manduriacu	65	343	−0.668	−79.426
Baba	42	187	−0.196	−78.429
Cumbayá	40	141	−1.430	−79.438
Sibimbe	15	94	−2.591	−78.567

6. Results and Discussions

The results regarding irradiance conditions, FPV system electrical performance, and water savings capabilities are summarized in Table 4 below. The FPV installation capacity is determined based on the available water space suitable for FPV deployment, as discussed in Section 5, where the upper limit is defined by the installed capacity of the HPP. This approach leverages the existing electrical transmission infrastructure of the HPP.

Table 4. Simulation results of HPP-FPV co-location for selected sites.

	Coca Codo Sinclair	Paute	Minas San Francisco	Marcel Laniado de Wind	Mazar	Agoyán	Pucará	Manduriacu	Baba	Cumbayá	Sibimbe
HPP capacity (MW)	1500	1100	270	213	170	154	70.6	65	42	40	15
Inclined irradiance (kWh/m ² /year)	1343	1448	1576	1335	1599	1509	1538	1272	1252	1895	1321
Average ambient temperature (°C)	16.8	14.1	20.3	22.9	14.2	15.2	7.0	20.6	21.9	13.4	22.1
FPV capacity (MWp)	53	160	51	213	170	6	70.6	55	42	17	15
FPV energy production (GWh/year)	58	182	61	6777	793	7	628	61	850	29	94
FPV contribution on HPP (%)	0.7	4.2	6.1	22.1	36.8	0.8	51.7	17.8	24.6	20.3	18.5
PR (%)	81.6	78.7	75.8	87.3	75.1	82.7	89.4	87.4	87.6	88.6	87.4
Yield (kWh/kWp)	1096	1139	1195	1165	1201	1248	1375	1113	1097	1678	1155
Far shading losses (%)	10.2	13.2	12.1	0.6	17.0	9.5	1.5	2.3	1.3	0.8	0.4
Soiling losses (%)	0.5	1.5	5.5	3.0	1.5	0.5	1.0	1.0	2.0	1.5	3.0
Module temperature losses (%)	2.4	1.7	3.2	3.6	1.9	2.1	0.0	3.2	3.3	2.2	3.5
Water savings (m/year)	0.69	0.74	0.84	0.78	0.76	0.70	0.70	0.73	0.71	0.80	0.73
Water savings (gallons/year)	1394	4498	1616	6321	4870	159	1864	1515	1124	515	413

Based on the table, the following insights can be drawn:

- The maximum FPV capacity, constrained by the selected water area and HPP capacity, indicates that the Marcel Laniado de Wind HPP offers the highest FPV installation

potential at 213 MWp, followed by Mazar (170 MWp) and Paute (160 MWp). All other installations are projected to have capacities below 100 MWp.

- In terms of weather conditions, the Cumbayá HPP experiences the highest overall irradiance reaching the solar panels (1895 kWh/m²/year), significantly surpassing other sites. Higher irradiance levels are expected to enhance the FPV yield.
- The most efficient system is located at the Pucará site, achieving a performance ratio (PR) of 89.4%, while Mazar records the lowest with a PR of 75.1%. These PR values are influenced by various loss factors associated with FPV system performance. Notably, far shading losses are significant at Mazar (17.0%) due to its mountainous surroundings, whereas the Minas San Francisco site exhibits the highest soiling losses (5.5%). Interestingly, Pucará shows the lowest module temperature losses (0.0%), likely attributable to its cooler ambient temperatures.
- With respect to water savings, the Marcel Laniado de Wind site produces the highest annual savings (6321 gallons/year), which is beneficial for HPP operations. Mazar (4870 gallons/year) and Paute (4498 gallons/year) also demonstrate significant savings. In terms of water savings per unit area, Minas San Francisco and Cumbayá exhibit the highest potential, at 0.84 m/year and 0.80 m/year, respectively.

Additionally, Figure 5 provides a comparison between the installation capacities of the hydropower plants (HPPs) and their corresponding floating photovoltaic (FPV) systems. The figure shows that for HPPs such as Marcel Laniado de Wind, Mazar, Pucará, and Baba, the FPV capacity was constrained to align with the HPP capacity to avoid exceeding the limits of the existing electrical infrastructure. In contrast, HPPs like Coca Codo Sinclair, Paute, Minas San Francisco, and Agoyán exhibit a significant gap between their potential FPV capacities and the existing HPP capacity. This difference could be advantageous, as it may help minimize any potential strain on the electrical infrastructure, ensuring that the FPV systems do not exert excessive pressure on the grid.

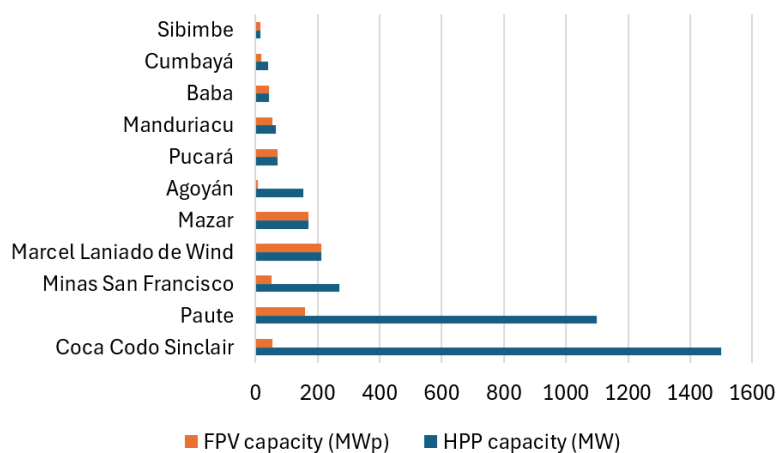


Figure 5. Installation capacity of FPV and HPP for the selected sites.

In Figure 6, the normalized values for energy production, performance ratio (PR), and yield are presented. It is evident that Marcel Laniado de Wind leads in energy production compared to the other systems, with Mazar and Paute following closely behind. This can be understood, as these achieve the highest FPV installation capacity among all sites. However, when assessing operational efficiency, Pucará stands out with the highest PR, which is comparable to most other systems. In contrast, Mazar and Minas San Francisco exhibit the lowest PR values, primarily due to significant losses from factors such as far shading and soiling. In terms of yield, Cumbayá takes the top spot, outperforming all other sites by a considerable margin. This exceptional performance is attributed to its high PR

value and optimal site conditions, including one of the highest inclined irradiance levels, which enhances the overall energy production potential.

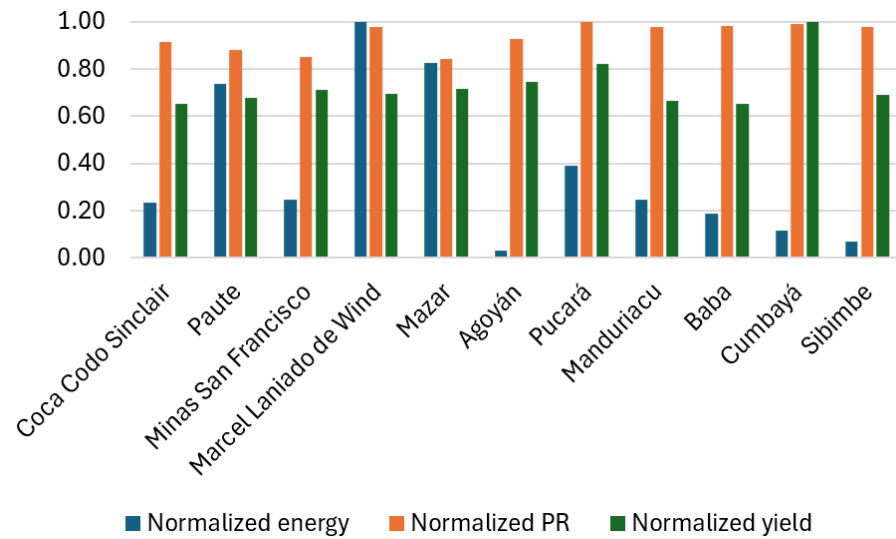


Figure 6. Normalized results for FPV energy production, performance ratio and yield.

Figure 7 presents the normalized water savings, both in terms of total volume (gallons) and based on the height (m) of the saved water. In terms of total water savings, the figure shows that Marcel Laniado de Wind, followed by Mazar and Paute, achieve the highest results. This is primarily due to the extensive coverage of water by their FPV systems, leading to the largest overall water savings. However, when evaluating the efficiency of water savings based on the height of the water saved beneath the FPV systems, Minas San Francisco ranks first, with the other systems falling within 17% of its performance. This suggests that while site conditions play a role in water savings, the key determinant is likely the extent of water covered by the FPV systems.

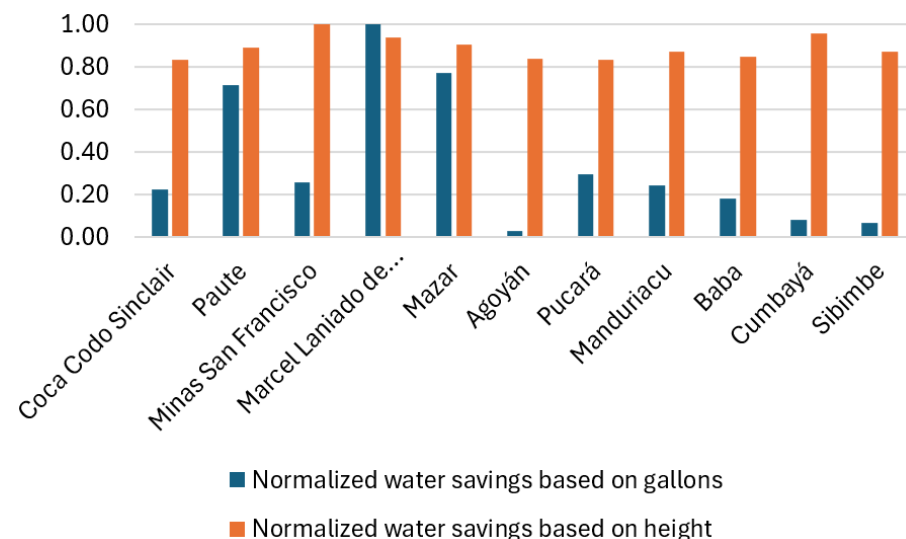


Figure 7. FPV normalized results related to the water savings based on total amount and height.

While the above results quantify the potential benefits of co-locating FPV systems with the analyzed HPPs, our goal is to rank these HPPs based on their overall FPV potential. We have identified three key parameters for this ranking: (a) maximum FPV capacity, (b) yield, and (c) water savings per unit area. An equal weighting index of 1/3 is applied to each of

these parameters, calculated using a linear approach where the lowest parameter value is set to 0% and the highest to 100%. The ranking based on this methodology is presented in Table 5 below. We acknowledge that other factors, such as electrical infrastructure conditions, proximity to population centers, and site accessibility, could also influence the ranking. Different weighting indices could be applied to these parameters based on their relative significance. However, a detailed analysis incorporating these additional factors would require further information beyond the scope of this study. Thus, the table should be regarded as a general guideline.

Table 5. Ranking of HPP sites based on their FPV advantage.

Ranking	HPP Site	FPV Capacity (MWp)
1	Cumbayá	17
2	Marcel Laniado de Wind	213
3	Mazar	170
4	Minas San Francisco	51
5	Paute	160
6	Pucará	70.6
7	Manduriacu	55
8	Sibimbe	15
9	Agoyán	6
10	Baba	42
11	Coca Codo Sinclair	53

Figure 8 then shows the geographical distribution of the 11 selected HPPs for FPV deployment, highlighting both their potential FPV capacity and energy production.

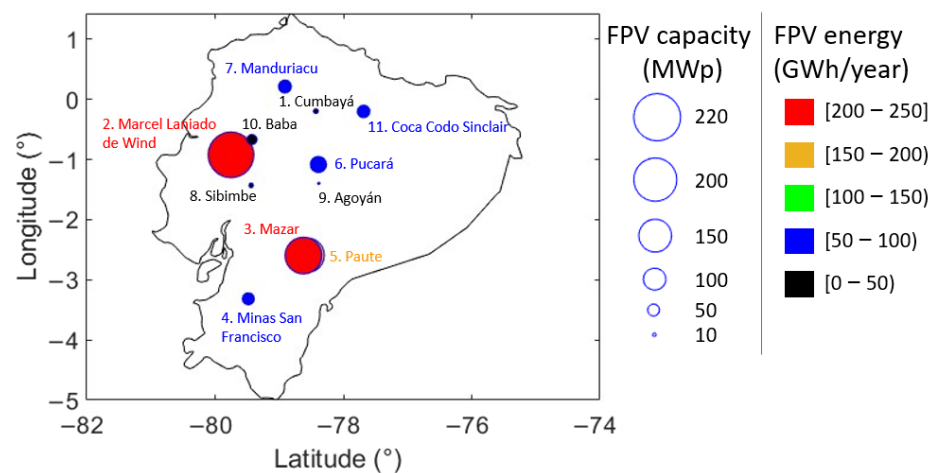


Figure 8. The map shows the locations of selected hydro power plants in Ecuador for potential FPV deployment. The size of each circle is proportional to the FPV installation capacity, while the color represents the FPV energy production potential. The names of the selected HPPs are also displayed, with each number corresponding to the FPV ranking based on this study. The color of the text matches the circle color for easy identification. Negative latitude values refer to the Western hemisphere while positive longitude values refer to the Northern hemisphere.

Given that the simulation results rely on inputs and methodologies that inherently carry uncertainties, we conducted an uncertainty analysis on the electrical performance of the FPV systems to better assess potential deviations. In this analysis, we used percentile calculations, where the P50 value represents the most likely outcome (also presented in Table 4). The P75 and P90 values indicate the performance levels that are expected to be exceeded, with probabilities of 75% and 90%, respectively. These estimations were made using a normal distribution based on the identified uncertainty values. The distribution

and corresponding percentile values are illustrated in Figure 9 below. Table 6 provides the *p* values, which highlight the reduction in performance at the P75 and P90 levels compared to the P50 value. These results offer additional insights into the range of expected FPV system performance, contributing to more robust and reliable expectations.

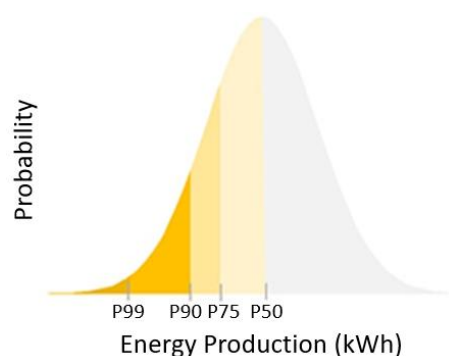


Figure 9. Normal statistical distribution showing the percentile values employed for the uncertainty analysis. Source: <https://eepower.com/>.

Table 6. Uncertainty results based on the P75 and P90 values.

	Coca Codo Sinclair	Paute	Minas San Francisco	Marcel Laniado de Wind	Mazar	Agoyán	Pucará	Manduriacu	Baba	Cumbayá	Sibimbe
FPV energy production (GWh/year)											
P50	58	182	61	6777	793	7	628	61	850	29	94
P75	55	168	56	6334	736	7	580	56	792	27	87
P90	52	156	52	5936	686	6	537	52	740	25	82
PR (%)											
P50	81.6	78.7	75.8	87.3	75.1	82.7	89.4	87.4	87.6	88.6	87.4
P75	77.2	72.7	70.0	81.6	69.8	76.1	82.6	80.6	81.6	82.8	81.6
P90	73.2	67.4	64.7	76.4	65.0	70.1	76.4	74.5	76.3	77.6	76.4
Yield (kWh/kWp)											
P50	1096	1139	1195	1165	1201	1248	1375	1113	1097	1678	1155
P75	1036	1053	1103	1089	1116	1148	1270	1026	1022	1569	1078
P90	983	976	1020	1021	1039	1058	1176	948	955	1470	1010

7. Conclusions

This paper explored the potential for co-locating floating photovoltaic (FPV) systems with hydropower plants (HPPs) in Ecuador. The findings highlight several advantages, including enhanced grid reliability and the ability of FPV systems to support HPPs during dry seasons, when hydropower generation is constrained. By sharing transmission infrastructure, FPV systems can improve operational efficiency while also reducing water evaporation, which benefits HPP performance.

Our analysis identified 11 HPPs in Ecuador with the capacity to host FPV systems exceeding 15 MWp. Based on the potential FPV installation capacity, electrical yield, and water savings; Cumbayá HPP emerged as the most favorable site for FPV deployment, with a maximum capacity of 17 MWp, followed closely by Marcel Laniado de Wind HPP (213 MWp) and Mazar HPP (170 MWp).

Additionally, we suggest exploring the potential for hybridization, where FPV and HPP systems operate together, optimizing energy output by coordinating FPV-generated power with HPP turbine operation. Challenges such as designing an effective control

system and evaluating infrastructure should also be addressed in future studies to fully realize the benefits of FPV-HPP integration.

Author Contributions: Conceptualization, C.D.R.-G. and O.G.; methodology, C.D.R.-G.; software, C.D.R.-G.; formal analysis, C.A.R.-G.; investigation, C.A.R.-G. and M.S.A.-A.; resources, C.D.R.-G.; data curation, C.D.R.-G. and O.G.; writing—original draft preparation, C.D.R.-G.; writing—review and editing, O.G., C.A.R.-G. and M.S.A.-A.; visualization, C.A.R.-G.; supervision, O.G.; project administration, C.D.R.-G. All authors have read and agreed to the published version of the manuscript.

Funding: This research received no external funding.

Institutional Review Board Statement: Not applicable.

Informed Consent Statement: Not applicable.

Data Availability Statement: The data presented in this study are available on request from the corresponding author due to intellectual property constraints.

Conflicts of Interest: The authors declare no conflict of interest.

References

1. Tkáč, Š. Hydro power plants, an overview of the current types and technology. *Sel. Sci. Pap.-J. Civ. Eng.* **2018**, *13*, 115–126. [CrossRef]
2. Tihomir, M.; Bryan, K.W.; Stanislav, P. Essential role of technical review in hydro-designs. In Proceedings of the 2009 IEEE Electrical Power & Energy Conference (EPEC), Montreal, QC, Canada, 22–23 October 2009; IEEE: Piscataway, NJ, USA, 2009; pp. 1–7.
3. Shang, Y.; Shang, L.; Li, X. *Technological Innovations and Advances in Hydropower Engineering*; Intech Open: London, UK, 2022; pp. 1–96. ISBN 978-1-83968-914-7.
4. Operador_Nacional_de_Electricidad_CENACE. *Informe Anual 2023*; Centro Nacional de Control de Energía de la República del Ecuador: Quito, Ecuador, 2023; pp. 1–103.
5. Singh, V.K.; Singal, S.K. Operation of hydro power plants—a review. *Renew. Sustain. Energy Rev.* **2017**, *69*, 610–619. [CrossRef]
6. Wasti, A.; Ray, P.; Wi, S.; Folch, C.; Ubierna, M.; Karki, P. Climate change and the hydropower sector: A global review. *Wiley Interdiscip. Rev. Clim. Change* **2022**, *13*, e757. [CrossRef]
7. CBS_NEWS. Ecuador Imposing Overnight Blackouts as Drought Saps Hydroelectric Power Capacity. 2024. Available online: <https://www.cbsnews.com/news/ecuador-blackouts-drought-hits-hydroelectric-power-capacity/> (accessed on 1 September 2024).
8. EL_PAIS. Severe Energy Crisis Paralyzes Ecuador for Two Days. 2024. Available online: <https://english.elpais.com/international/2024-04-18/severe-energy-crisis-paralyzes-ecuador-for-two-days.html> (accessed on 1 September 2024).
9. EL_PAIS. Massive Blackout Leaves Ecuador Without Power for over Three Hours. 2024. Available online: <https://english.elpais.com/international/2024-06-20/massive-blackout-leaves-ecuador-without-power-for-over-three-hours.html> (accessed on 1 September 2024).
10. Rodríguez-Gallegos, C.; Gandhi, O.; Reindl, T.; Panda, S. PHSO: A graphic user interface optimizer for the sizing design of the PV hybrid systems. In Proceedings of the 33rd European Photovoltaic Solar Energy Conference and Exhibition (EUPVSEC), Amsterdam, The Netherlands, 25–29 September 2017; pp. 2375–2379.
11. Rodríguez-Gallegos, C.D.; Yang, D.; Gandhi, O.; Bieri, M.; Reindl, T.; Panda, S. A multi-objective and robust optimization approach for sizing and placement of PV and batteries in off-grid systems fully operated by diesel generators: An Indonesian case study. *Energy* **2018**, *160*, 410–429. [CrossRef]
12. Rodríguez-Gallegos, C.D.; Gandhi, O.; Bieri, M.; Reindl, T.; Panda, S. A diesel replacement strategy for off-grid systems based on progressive introduction of PV and batteries: An Indonesian case study. *Appl. Energy* **2018**, *229*, 1218–1232. [CrossRef]
13. Gallegos, C.D.R. *Modelling and Optimization of Photovoltaic Cells, Modules, and Systems*; Springer Nature: Berlin/Heidelberg, Germany, 2021; Springer Theses; pp. 1–153. ISSN 2190-5053.
14. Rodríguez-Gallegos, C.D.; Vinayagam, L.; Gandhi, O.; Yagli, G.M.; Alvarez-Alvarado, M.S.; Srinivasan, D.; Reindl, T.; Panda, S. Novel forecast-based dispatch strategy optimization for PV hybrid systems in real time. *Energy* **2021**, *222*, 119918. [CrossRef]
15. Rodríguez-Gallegos, C.D.; Gandhi, O.; Sun, H.; Paton, C.; Zhang, J.; Ali, J.M.Y.; Alvarez-Alvarado, M.S.; Zhang, W.; Rodríguez-Gallegos, C.A.; Chua, L.H.; et al. Global floating PV status and potential. *Prog. Energy* **2024**, *7*, 015001. [CrossRef]
16. International_Energy_Agency. *Snapshot of Global PV Markets 2024*; International Energy Agency: Paris, France, 2024; pp. 1–25.

17. Fuchs, R.; Bawono, A.A.; Lechner, B.; Rodríguez-Gallegos, C.D. Solar Photovoltaic Potential for Ballastless and Ballasted Railway Tracks: A Singapore Case Study. *Soc. Sci. Res. Netw.* **2024**, *10*, 1–36.
18. Gallegos, C.R.; Walsh, T.M. Conceptual design for a stand-alone solar photovoltaic powered peltier air conditioner. In Proceedings of the World Engineer’s Summit (WES) on Climate Change, Singapore, 21–24 July 2015.
19. Rodríguez Gallegos, C.D.; Rodríguez Gallegos, C.D. Optimal Diesel Replacement Strategy for the Progressive Introduction of PV and Batteries. In *Modelling and Optimization of Photovoltaic Cells, Modules, and Systems*; Springer: Singapore, 2021; pp. 83–110.
20. Garces-Palacios, L.E.; Rodríguez-Gallegos, C.D.; Vaca-Urbano, F.; Alvarez-Alvarado, M.S.; Gandhi, O.; Rodríguez-Gallegos, C.A. Optimal Design of a Hybrid Solar–Battery–Diesel System: A Case Study of Galapagos Islands. *Solar* **2024**, *4*, 232–245. [[CrossRef](#)]
21. Luo, W.; Khoo, Y.S.; Hacke, P.; Jordan, D.; Zhao, L.; Ramakrishna, S.; Aberle, A.G.; Reindl, T. Analysis of the long-term performance degradation of crystalline silicon photovoltaic modules in tropical climates. *IEEE J. Photovolt.* **2018**, *9*, 266–271. [[CrossRef](#)]
22. Luo, W.; Khaing, A.M.; Rodriguez-Gallegos, C.D.; Leow, S.W.; Reindl, T.; Pravettoni, M. Long-term outdoor study of an organic photovoltaic module for building integration. *Prog. Photovolt. Res. Appl.* **2024**, *32*, 481–491. [[CrossRef](#)]
23. Zhao, S.; Low, Y.M.; Rodríguez-Gallegos, C.D.; Reindl, T. Potential root causes for failures in floating PV systems. In Proceedings of the International Conference on Offshore Mechanics and Arctic Engineering, Melbourne, Australia, 11–16 June 2023; American Society of Mechanical Engineers: New York, NY, USA; Volume 86908, p. V008T009A012.
24. Solomin, E.; Sirotkin, E.; Cuce, E.; Selvanathan, S.; Kumarasamy, S. Hybrid Floating Solar Plant Designs: A Review. *Energies* **2021**, *14*, 2751. [[CrossRef](#)]
25. Ahmad, K.; Rahman, A. Feasibility Analysis of Floating Solar PV Project in Catchment Area of Kaptai Dam. In Proceedings of the 2022 International Conference on Energy and Power Engineering (ICEPE), Shillong, India, 29 April–1 May 2022; IEEE: Piscataway, NJ, USA, 2022; pp. 1–5.
26. Mamatha, G.; Kulkarni, P. Assessment of floating solar photovoltaic potential in India’s existing hydropower reservoirs. *Energy Sustain. Dev.* **2022**, *69*, 64–76. [[CrossRef](#)]
27. Waewsak, J.; Ali, S.; Natee, W.; Kongruang, C.; Chancham, C.; Gagnon, Y. Assessment of hybrid, firm renewable energy-based power plants: Application in the southernmost region of Thailand. *Renew. Sustain. Energy Rev.* **2020**, *130*, 109953. [[CrossRef](#)]
28. Ali, S.; Taweekun, J.; Techato, K.; Waewsak, J.; Gyawali, S. GIS based site suitability assessment for wind and solar farms in Songkhla, Thailand. *Renew. Energy* **2019**, *132*, 1360–1372. [[CrossRef](#)]
29. Santos, F.R.d.; Wiecheteck, G.K.; Virgens Filho, J.S.d.; Carranza, G.A.; Chambers, T.L.; Fekih, A. Effects of a floating photovoltaic system on the water evaporation rate in the passaúna reservoir, Brazil. *Energies* **2022**, *15*, 6274. [[CrossRef](#)]
30. Benjamins, S.; Williamson, B.; Billing, S.-L.; Yuan, Z.; Collu, M.; Fox, C.; Hobbs, L.; Masden, E.A.; Cottier-Cook, E.J.; Wilson, B. Potential environmental impacts of floating solar photovoltaic systems. *Renew. Sustain. Energy Rev.* **2024**, *199*, 114463. [[CrossRef](#)]
31. Egler, M.; Rusbridge, S.; Santos, C. Solar Resource Databases vs Weighted Means—Results Of A Global Benchmarking Effort. In Proceedings of the 4th International Conference Energy Meteorology, Bari, Italy, 27–29 June 2017.
32. Meteonorm. Meteonorm Software: Worldwide Irradiation Data. 2024. Available online: <https://meteonorm.com/en/> (accessed on 1 September 2024).
33. Solargis. Most Accurate Data and Software for PV Plant Investments. 2024. Available online: <https://solargis.com/> (accessed on 1 September 2024).
34. National_Renewable_Energy_Laboratory. NSRDB: National Solar Radiation Database. 2024. Available online: <https://nsrdb.nrel.gov/> (accessed on 1 September 2024).
35. PVSyst. A Full Package for the Study of Your Photovoltaic Systems. 2024. Available online: <https://www.pvsyst.com/> (accessed on 1 September 2024).
36. Rodríguez-Gallegos, C.D.; Bieri, M.; Gandhi, O.; Singh, J.P.; Reindl, T.; Panda, S. Monofacial vs bifacial Si-based PV modules: Which one is more cost-effective? *Sol. Energy* **2018**, *176*, 412–438. [[CrossRef](#)]
37. Rodríguez-Gallegos, C.D.; Liu, H.; Gandhi, O.; Singh, J.P.; Krishnamurthy, V.; Kumar, A.; Stein, J.S.; Wang, S.; Li, L.; Reindl, T.; et al. Global techno-economic performance of bifacial and tracking photovoltaic systems. *Joule* **2020**, *4*, 1514–1541. [[CrossRef](#)]
38. LONGi. *Installation Manual for LONGi Solar PV Modules*; LONGi: Xi’an, China, 2024; pp. 1–29.
39. Trina_Solar. *Trina Solar User Manual*; Trina Solar: Changzhou, China, 2024; pp. 1–37.
40. World_Bank_Group; ESMAP; SERIS. *Where Sun Meets Water: Floating Solar Handbook for Practitioners*; World Bank: Washington DC, USA, 2019; pp. 1–155.
41. Rodríguez-Gallegos, C.D.; Gandhi, O.; Panda, S.; Reindl, T. On the PV tracker performance: Tracking the sun versus tracking the best orientation. *IEEE J. Photovolt.* **2020**, *10*, 1474–1480. [[CrossRef](#)]
42. Micheli, L. The temperature of floating photovoltaics: Case studies, models and recent findings. *Sol. Energy* **2022**, *242*, 234–245. [[CrossRef](#)]
43. Wu, H.-P.; Tseng, C.-Y.; Jen, C.-C.; Chiang, Y.-C.; Chen, S.-L. Analysis of the Potential for Enhancing the Efficiency of a Floating Photovoltaic (FPV) System. *J. Mar. Sci. Technol.* **2024**, *32*, 7. [[CrossRef](#)]

44. Sukarso, A.P.; Kim, K.N. Cooling effect on the floating solar PV: Performance and economic analysis on the case of west Java province in Indonesia. *Energies* **2020**, *13*, 2126. [[CrossRef](#)]
45. Dörenkämper, M.; Wahed, A.; Kumar, A.; de Jong, M.; Kroon, J.; Reindl, T. The cooling effect of floating PV in two different climate zones: A comparison of field test data from the Netherlands and Singapore. *Sol. Energy* **2021**, *219*, 15–23. [[CrossRef](#)]
46. Dörenkämper, M.; Van den Werf, D.; Sinapis, K.; De Jong, M.; Folkerts, W. Influence of wave induced movements on the performance of floating pv systems. In Proceedings of the 36th European Photovoltaic Solar Energy Conference (EUPVSEC), Marseille, France, 9–13 September 2019; pp. 1759–1762.
47. Rosa-Clot, P. FPV and environmental compatibility. In *Floating PV Plants*; Elsevier: Amsterdam, The Netherlands, 2020; pp. 101–118.
48. Ziar, H.; Prudon, B.; Lin, F.Y.; Roeffen, B.; Heijkoop, D.; Stark, T.; Teurlinx, S.; de Senerpont Domis, L.; Goma, E.G.; Extebarria, J.G.; et al. Innovative floating bifacial photovoltaic solutions for inland water areas. *Prog. Photovolt. Res. Appl.* **2021**, *29*, 725–743. [[CrossRef](#)]
49. Zhang, W.; Liu, S.; Gandhi, O.; Rodríguez-Gallegos, C.D.; Quan, H.; Srinivasan, D. Deep-learning-based probabilistic estimation of solar PV soiling loss. *IEEE Trans. Sustain. Energy* **2021**, *12*, 2436–2444. [[CrossRef](#)]
50. Zhang, W.; Archana, V.; Gandhi, O.; Rodríguez-Gallegos, C.D.; Quan, H.; Yang, D.; Tan, C.-W.; Chung, C.; Srinivasan, D. SoilingEdge: PV Soiling Power Loss Estimation at the Edge Using Surveillance Cameras. *IEEE Trans. Sustain. Energy* **2023**, *15*, 556–566. [[CrossRef](#)]
51. Linacre, E.T. A simple formula for estimating evaporation rates in various climates, using temperature data alone. *Agric. Meteorol.* **1977**, *18*, 409–424. [[CrossRef](#)]

Disclaimer/Publisher’s Note: The statements, opinions and data contained in all publications are solely those of the individual author(s) and contributor(s) and not of MDPI and/or the editor(s). MDPI and/or the editor(s) disclaim responsibility for any injury to people or property resulting from any ideas, methods, instructions or products referred to in the content.